INTERNATIONAL JOURNAL OF
NUMERICAL ANALYSIS AND MODELING
Volume 3, Number 4, Pages 377–394

TOWARDS A LEVEL SET FRAMEWORK FOR INFARCTION MODELING: AN INVERSE PROBLEM

MARIUS LYSAKER AND BJØRN FREDRIK NIELSEN

Abstract. The purpose of this paper is to introduce a level set framework suitable for identifying heart infarctions. We do this by introducing a modified Monodomain model, and an output least squares formulation comparing simulation results with observation data. In this way we obtain a flexible methodology allowing us to approximately determine the characteristics of infarctions with rather complex geometrical properties. Our approach involves a CPU demanding minimization problem. This problem is solved by applying an adjoint equation enabling efficient differentiation of the involved cost-functional. Finally, our theoretical findings are illuminated by a series of numerical experiments.

Key Words. Level set, Monodomain model, heart infarctions and inverse problems.

1. Introduction

Heart conditions are among the most widespread illnesses in the Western world, and cause the deaths of millions of people every year. The main purpose of this paper is to study one of these conditions, heart infarctions; or more generally, ischemic heart illnesses. Our approach will not follow the methods of contemporary medical research, but will instead investigate the possibilities for using modern computational mathematics and high speed computers to gain insight into this growing health problem.

When a coronary artery, which supplies blood to the heart, becomes blocked, the heart muscle does not receive adequate blood and oxygen. Ultimately, this can result in the death of the heart tissue, a condition known as a heart infarction. Ischemia is a precursor of infarction, i.e. if the ischemic condition (lack of blood) persists, the outcome will be an infarction. Therefore, one might characterize an ischemia as a mild and reversible form of infarction. For the sake of simplicity, we will throughout this text use these two terms synonymously.

The first electrocardiogram (ECG) was recorded by Waller in 1887. It is difficult to exaggerate the importance of this discovery. Nowadays, millions of ECGs are recorded every day around the world. It is by far the most commonly used tool to identify ischemic heart disease. This is probably due to its simplicity, reliability, and the relatively low costs associated with buying and maintaining an electrocardiograph. However, despite its apparent success, the traditional human expert-based procedure for interpreting ECG recordings has its weaknesses; in many cases the

Received by the editors September 1, 2004 and, in revised form, March 19, 2005.
2000 *Mathematics Subject Classification.* 35R30, 49Q10, 65N21.

procedure simply fails to detect an ischemia, see Lau et.al. [22]. Moreover, ECG recordings provide only a rather crude picture of the position and size of infarctions, cf. Birnbaum and Drew [2]. Thus, there is a need to improve this technology further.

The electrical activity in the human heart is governed by the Bidomain equations. This model was introduced by Tung [40] and has been studied by many authors; see [28, 25, 24] and references given therein. A general introduction is presented in [20].

In [38] a rather abstract and general method for including the effect of ischemic heart disease into the Bidomain equations was suggested. Furthermore, a methodology for identifying heart infarctions, in terms of an output least squares framework, was proposed and analyzed. However, among several unsolved challenges, this study did not provide any answer to the following important problem:

(1) *How can the possibly complex geometrical properties of infarctions be incorporated into such mathematical models?*

The purpose of the present paper is to shed some light onto this problem. Some initial considerations on how to handle (1) for a rather idealized model will be presented. More precisely, we propose to apply a level set methodology to include the effect of ischemic tissues into the equations. This enables us to formulate a flexible framework for identifying heart infarctions. Expressed in mathematical terms, the ischemic region is recovered by solving an inverse problem for a partial differential equation (PDE). That is, boundary measurements of the solution of the PDE is applied to identify an unknown coefficient in the equation. This unknown coefficient, as well as the involved conductivities, are parameterized in terms of a level set technique.

The Bidomain model consists of a coupled system of PDEs. Their efficient numerical solution is a very difficult scientific issue, typically involving extremely CPU demanding algorithms - see [37]. As mentioned above, the main purpose of the present paper is to propose a method for incorporating the possibly complex geometrical structures of infarctions into models of the electrical activity in the heart. For the sake of simplicity, we will therefore focus on the less physically accurate Monodomain model[1]. The Monodomain model consists of a scalar parabolic PDE. It can therefore be solved efficiently by standard numerical methods for parabolic problems. Hence, this equation is well-suited for a conceptually study of the problem posed in (1).

Several scientists have analyzed inverse problems that arise in connection with ECG recordings. In particular, the problem of computing the epicardial potential, i.e. the electrical potential at the surface of the heart, from body surface measurements has received a lot of attention. (See, e.g. Franzone, Taccardi and Viganotti [10], MacLeod and Brooks [27], Dössel [7] and Greensite and Huiskamp [11], to mention a few.) Roughly speaking, the goal of such studies is to compute ECG recordings for the surface of the heart, and thereby obtain a deeper understanding of this organ. This task may be formulated in terms of a single linear elliptic partial

[1]The Monodomain model can be derived from the Bidomain equations by assuming that the involved extra and intra -cellular conductivities are proportional quantities, see [20, 38] for further details. We hope to treat the Bidomain case in our future work.

differential equation. Due to its severe ill-posed nature, it is a difficult problem to solve, but the computational demands are relatively moderate.

The challenge of how to combine ECG recordings with mathematics and computations to identify ischemic heart disease has by far received the same kind of attention. In fact, as far as the authors know, only a few texts dealing with this topic exist; in [16, 15, 29, 18, 19, 21, 23, 14] and [26] the effect of infarctions on ECG signals is studied from a simulation point of view, and in [38] a suitable parameter estimation problem is presented. On the other hand, applying level set techniques for identifying complex geometrical structures in terms of inverse problems has become quite popular throughout the last decade, see [32, 5, 3, 39]. An interesting and related work is the approach presented in [6]. In that paper, the authors utilize a level set framework to represent interfaces between domains with different conductivity coefficients for a problem arising in connection with electrical impedance tomography.

The outline for the rest of this paper is as follows. The main purpose of Section 2 is to derive a suitable mathematical model problem, including methods for incorporating the effects of ischemic regions. As mentioned above, the novelty of this work is to utilize a level set technique in the framework. In order to estimate the size, shape and location of the infarction from ECG recordings, a minimization problem must be solved. This is the topic for Section 3, including an efficient method for computing the gradient of the involved cost-functional. In this section we also outline an algorithm. Due to the ill-posedness of this inverse problem, we need to regularize the solution, and different regularization techniques are therefore presented in Section 4. In Section 5 we present several numerical experiments, followed by some conclusions in Section 6.

2. A model problem

Throughout this paper we will consider the Monodomain model for the electrical activity in the heart:

$$\chi C v_t + \chi I_{\text{ion}} = \nabla \cdot (K \nabla v) \qquad \text{in } \Omega, \tag{2}$$

$$(K \nabla v) \cdot n = 0 \qquad \text{along } \partial\Omega, \tag{3}$$

$$v(x, 0) = v_0(x) \qquad \text{in } \Omega, \tag{4}$$

cf. [20]. In these equations, v represents the membrane potential, and Ω the physical domain occupied by the heart. The cellular conductivity tensor K is typically defined in terms of a symmetric and positive definite matrix depending on the spatial position x. The ionic current is incorporated into the model by the possibly nonlinear function I_{ion}, and χ and C are given constants[2].

Equations (2)-(4) model the electrical activity in an insulated heart, cf. the boundary condition (3). In more realistic simulations, this model must be coupled to an equation governing the potential in the remaining part of the body, i.e. in the region outside the heart - see [38]. Our long term goal is to derive a flexible framework for identifying ischemic heart disease. The present paper, being an initial investigation of the possibilities for doing so, should focus on a simple model

[2]More precisely, χ represents the the area of cell membrane per unit volume, and C denotes the capacitance of the cell membrane.

problem. We therefore only consider the heart, denoted by Ω, and assume that ECGs can be recorded at the entire epicardial surface $\partial\Omega$.

By defining

$$\begin{aligned} I &= \frac{1}{C} I_{\text{ion}}, \\ k &= \frac{1}{\chi C} K, \end{aligned}$$

we may write (2)-(4) on the form

$$v_t + I(v) = \nabla \cdot [k \nabla v] \qquad \text{in } \Omega, \tag{5}$$

$$(k \nabla v) \cdot n = 0 \qquad \text{along } \partial\Omega, \tag{6}$$

$$v(x, 0) = v_0(x) \qquad \text{in } \Omega. \tag{7}$$

Throughout this text we will refer to k as the conductivity, even though it strictly speaking is a "scaled" conductivity.

Typically, the ionic current I across the cell membrane is a nonlinear function of the membrane potential v, as well as of the intra-cellular ionic concentrations and the gate variables related to the cell dynamics. However, for the sake of simplicity, we will assume that I only depends on the potential v and that it is given by a cubic model:

$$I(v) = -A^2(v + v_{\text{rest}})(v + v_{\text{th}})(v - v_{\text{peak}}), \tag{8}$$

see [17] for details. In this model, A, v_{rest}, v_{th} and v_{peak} are given constants.

Equations (5)-(7) simulate the electrical potential within a healthy heart. In order to model the effect of infarctions we must modify this model. To do so, we introduce the parameters

$$p_1, p_2, \ldots, p_M \tag{9}$$

to represent the geometrical characteristics of the ischemic region. These variables will in the following be referred to as the *infarction parameters*. At the present stage, this parameterization is abstract. The main purpose of this paper is to show how such a parameterization can be realized in terms of a level set framework. Furthermore, we will use this methodology to identify infarctions. These topics are treated in detail in sections 2.2-3.2 below.

According to biological observations, the cells in an infarcted area are not excitable, and the conductivity differs compared with healthy regions [13, 36]. Consequently, an ischemia can be incorporated into the model (5)-(7) by diverting (forcing) the ion transport to go around the infarcted areas, and by changing the conductivity in such regions.

A pilot approach to simulate a blocking ion transport was proposed in [38]. The term $I(v)$ in (5) was replaced by $gI(v)$, where the function $g = g(x; p_1, p_2, \ldots, p_M)$ is zero (or close to zero) in the infarcted region, and equal to one elsewhere. A typical choice would be to define g as a step function:

$$g(x; p_1, p_2, \ldots, p_M) = \begin{cases} 0 & \text{if } x \text{ in } D, \\ 1 & \text{if } x \text{ in } \Omega \setminus D, \end{cases} \tag{10}$$

where D denotes the infarcted area of the heart. Above we introduced the variables $p_1, p_2, \ldots, p_M$ to represent the geometrical properties of the ischemic region. This

means that D is parameterized in terms of $p_1, p_2, \ldots, p_M$, i.e.

$$D = D(p_1, p_2, \ldots, p_M).$$

Our goal is to show how D can be discretized in terms of $p_1, p_2, \ldots, p_M$, and to use such methods to identify ischemia. As mentioned above, we will return to this issue in sections 2.2-2.4.

In a similar manner, the properties of the conductivity function k will also depend on whether or not infarctions are present, i.e.

$$k = k(x; p_1, p_2, \ldots, p_M).$$

Let us therefore introduce the notation

$$k(x; p_1, p_2, \ldots, p_M) = \begin{cases} k_1(x) & \text{if } x \text{ in } D, \\ k_2(x) & \text{if } x \text{ in } \Omega \setminus D, \end{cases} \tag{11}$$

where k_1 and k_2 are assumed to be given functions, see [13, 36] for further details.

With this notation at hand, we introduce the following model for the electrical potential in a heart Ω with an infarction D

$$v_t + gI(v) = \nabla \cdot [k \nabla v] \qquad \text{in } \Omega \tag{12}$$

$$k \nabla v \cdot n = 0 \qquad \text{along } \partial\Omega \tag{13}$$

$$v(x, 0) = v_0(x) \qquad \text{in } \Omega, \tag{14}$$

where $I(v)$ in (5) has been replaced by $gI(v)$. Note that the solution v of (12)-(14) depends on $D = D(p_1, p_2, \ldots, p_M)$, i.e.

$$v = v(x, t; p_1, p_2 \ldots, p_M).$$

2.1. The direct and inverse problem. Assume that the geometrical properties of the infarction D is known, i.e. $p_1, p_2 \ldots, p_M$ are given. Then we can easily solve (12)-(14) and compute the effect of this ischemia on the ECG at $\partial\Omega$. In the present setting, this is the direct problem.

However, this is not what we want to do. Our goal is to try to determine the unknown size, shape and location of D from boundary measurements of the membrane potential $v(x, t; p_1, p_2, \ldots, p_M)$, i.e. measurements at $\partial\Omega$. This is an inverse problem.

In order to do so, we will use an output least squares method. Let us therefore introduce the cost-functional

$$J(p_1, p_2, \ldots, p_M) = \frac{1}{2} \int_0^{t^*} \int_{\partial\Omega} \left[d(x, t) - v(x, t; p_1, p_2 \ldots, p_M) \right]^2 dx\, dt, \tag{15}$$

where $d(x, t)$ denotes the real world ECG data[3]. Here, $[0, t^*]$ is the time-interval under consideration.

For a given set of infarction parameters $\{p_i\}_{i=1}^M$, (15) measures the deviation between the observation data $d(x, t)$ and the simulated results at the boundary $\partial\Omega$ (obtained by solving (12)-(14)). The basic approach for finding a best fitted solution of (15), is to solve a minimization problem with respect to the infarction parameters

$$\min_{p_1, p_2, \ldots, p_M} J(p_1, p_2, \ldots, p_M). \tag{16}$$

[3]Throughout this text we assume that the ECG is recorded at the entire heart surface $\partial\Omega$. In practice, ECGs are only recorded at specific locations on the surface of the body, referred to as the leads.

That is, we consider an output least squares method.

The identification of parameters and coefficients in PDEs from boundary measurements of the solution is well-known to lead to ill-posed problems, see [1, 12]. Therefore, we expect (16) to be ill-posed, and consequently hard to solve. Further, an infarction might hold a nontrivial geometry, meaning that a large number of parameters are needed to represent the characteristics of the infarction. We now turn our attention towards this problem. In Section 3 an algorithm for approximately solving (16) is presented.

2.2. Implicit curves and surfaces. Our goal is to derive a flexible parameterization of the ischemic region D in terms of the infarction parameters $p_1, p_2 \ldots, p_M$. In order to do so, let us first recapture some simple facts about implicit curves and surfaces.

Let Γ be a closed curve in $\mathbb{R}^2$, or a closed surface in $\mathbb{R}^3$. If ϕ is a function such that

$$\text{(17)} \qquad \begin{cases} \text{if } \phi(x) < 0 & \Rightarrow \quad \text{x is inside } \Gamma, \\ \text{if } \phi(x) = 0 & \Rightarrow \quad \text{x is at } \Gamma, \\ \text{if } \phi(x) > 0 & \Rightarrow \quad \text{x is outside } \Gamma, \end{cases}$$

then Γ is implicitly represented by ϕ, in the sense that

$$\Gamma = \{x;\ \phi(x) = 0\}.$$

It is common to refer to ϕ as a level set function. In Figure 1(a) a simple level set function is illustrated, and its associated zero level set Γ is depicted in Figure 1(b).

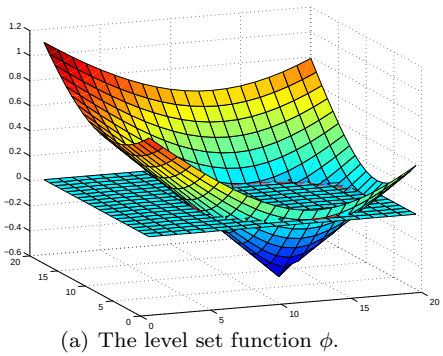

(a) The level set function ϕ.

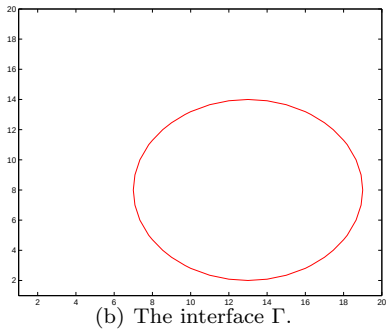

(b) The interface Γ.

FIGURE 1. A level set function ϕ and its zero level set $\Gamma = \{x;\ \phi(x) = 0\}$.

For a given curve Γ, there are of course infinitely many functions satisfying (17). Therefore, ϕ is usually defined by the following formula[4]

$$\text{(18)} \qquad \begin{cases} \phi(x) = -\ \text{dist}(\Gamma, \text{x}) & \text{if x is inside } \Gamma, \\ \phi(x) = \quad 0 & \text{if x is at } \Gamma, \\ \phi(x) = \quad \text{dist}(\Gamma, \text{x}) & \text{if x is outside } \Gamma, \end{cases}$$

[4]This is a delicate issue, depending on the application under consideration. Normally, some regularity must be imposed on ϕ to prevent the level set function of being too steep or too flat near Γ. It turns out that (18) provides a suitable solution to this kind of problems, see [31, 30, 35] for details.

where dist(Γ, x) denotes Euclidean distance between Γ and x. By applying definition (18), we obtain a one to one correspondence between Γ and the function ϕ.

The level set method was proposed by Osher and Sethian in [33] as a versatile tool for tracing interfaces separating a domain into subdomains. We have only scratched the surface of this field. Today it consists of a large tool-box, as well as a theory, for adding dynamics to implicit curves and surfaces, see e.g. [31, 3, 30, 35, 39] for further details.

2.3. A level set framework. Let us now turn our attention towards the model problem (12)-(14); more specifically, on how to describe the infarcted region D in terms of the parameters $p_1, p_2 \ldots, p_M$. In order to do so, we must somehow discretize the ideas briefly outlined above.

To this end, we will assume that a finite element mesh, with associated linear basis functions $\{N_i(x)\}_{i=1}^M$ and nodes $\{x_j\}_{j=1}^N$, has been defined on Ω, i.e. on the heart. Then we may introduce the discrete level set function

$$\phi = \phi(x; p_1, p_2 \ldots, p_M) = \sum_{i=1}^{M} p_i N_i(x), \tag{19}$$

where $p_1, p_2 \ldots, p_M$ denote the infarction parameters. In the discrete case, formula (18) takes the form

$$\begin{cases} \phi(x_j) = -\operatorname{dist}(\Gamma, \mathrm{x_j}) & \text{if } x_j \text{ is in } D, \\ \phi(x_j) = \quad 0 & \text{if } x_j \text{ is at } \partial D, \\ \phi(x_j) = \quad \operatorname{dist}(\Gamma, \mathrm{x_j}) & \text{if } x_j \text{ is outside } D, \end{cases} \tag{20}$$

for $j = 1, 2, \ldots, N$. Note that the boundary ∂D of the ischemic region D is approximately given by the zero level set of ϕ, i.e.

$$\partial D \approx \{x;\ \phi(x) = 0\}.$$

The quality of this approximation depends on both the underlying finite element mesh used to discretize ϕ, as well as the geometrical structure of D.

Next, let H denote the Heaviside function:

$$H(x) = \begin{cases} 0 & x < 0, \\ 1 & x \geq 0. \end{cases}$$

With this notation at hand, we may define the functions g and k in (10) and (11) as follows

$$g(x; p_1, p_2 \ldots, p_M) = H(\phi(x; p_1, p_2 \ldots, p_M)) \approx \begin{cases} 0 & \text{if } x \text{ in } D, \\ 1 & \text{if } x \text{ in } \Omega \setminus D, \end{cases} \tag{21}$$

and

$$k(x; p_1, p_2 \ldots, p_M) = k_1(1 - H(\phi)) + k_2 H(\phi) \approx \begin{cases} k_1(x) & \text{if } x \text{ in } D, \\ k_2(x) & \text{if } x \text{ in } \Omega \setminus D. \end{cases} \tag{22}$$

From a modeling point of view, (21)-(22) is an unrealistic method for distinguishing between healthy and infarcted tissues. A more realistic model should include a smooth transmission between these regions [34]. Such a border-zone can easily be incorporated into (21) and (22) in a cunning way by making use of a smooth

Heaviside function (and for later computations we also need the associated smooth Delta δ function):

$$H_\alpha(x) = \frac{1}{2} + \frac{1}{\pi}\tan^{-1}\Big(\frac{x}{\alpha}\Big),$$
$$\delta_\alpha(x) = H'_\alpha(x) = \frac{1}{\pi}\Big(\frac{\alpha}{\alpha^2 + x^2}\Big), \tag{23}$$

where $\alpha > 0$ incorporates the qualities of the border-zone between the healthy and infarcted regions. As $\alpha \to 0$, the approximations in (23) converge towards H and δ, respectively. Figure 2 shows the exact and smoothed Heaviside functions $H(x)$ and $H_\alpha(x)$, as well as $\delta_\alpha(x)$, for $\alpha = 0.5$.

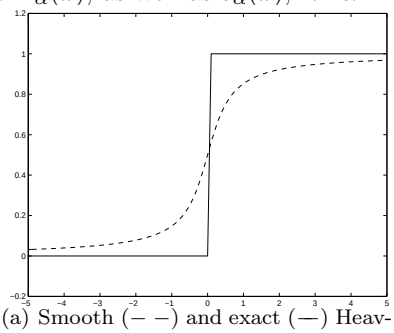

(a) Smooth (– –) and exact (—) Heaviside functions

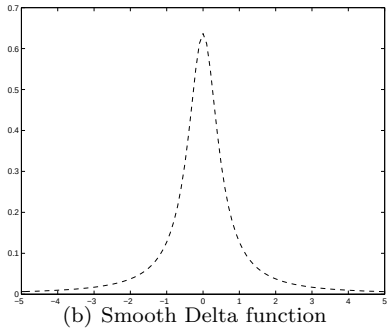

(b) Smooth Delta function

FIGURE 2. A smooth approximation of the Heaviside H and the Delta function δ. See [4] for further approximations of H and δ.

To include a border-zone in the modeling process, we replace $H(\phi)$ by $H_\alpha(\phi)$ in both (21) and (22) and use the notation $g_\alpha(\phi)$ and $k_\alpha(\phi)$ for these approximations:

$$g_\alpha(\phi) = H_\alpha(\phi) \approx \begin{cases} 0 & \text{if } x \text{ in } D, \\ 1 & \text{if } x \text{ in } \Omega \setminus D, \end{cases} \tag{24}$$

and

$$k_\alpha(\phi) = k_1(1 - H_\alpha(\phi)) + k_2 H_\alpha(\phi) \approx \begin{cases} k_1(x) & \text{if } x \text{ in } D, \\ k_2(x) & \text{if } x \text{ in } \Omega \setminus D, \end{cases} \tag{25}$$

where

$$\phi = \phi(x;\ p_1, p_2 \ldots, p_M) = \sum_{i=1}^{M} p_i N_i(x). \tag{26}$$

2.4. The complete problem. The complete form of the minimization problem (16) can now be written on the form

$$\min_{p_1,p_2,\ldots,p_M} J(p_1, p_2, \ldots, p_M) =$$
$$\min_{p_1,p_2,\ldots,p_M} \left(\frac{1}{2} \int_0^{t^*} \int_{\partial\Omega} \big[d(x,t) - v(x,t;p_1,p_2\ldots,p_M)\big]^2 dx\, dt \right) \tag{27}$$

subject to the constraint that v solves

$$v_t + g_\alpha(\phi) I(v) = \nabla \cdot [k_\alpha(\phi)\nabla v] \qquad \text{in } \Omega, \tag{28}$$
$$k_\alpha(\phi)\nabla v \cdot n = 0 \qquad \text{along } \partial\Omega, \tag{29}$$
$$v(x,0) = v_0(x) \qquad \text{in } \Omega, \tag{30}$$

and that

$$\begin{cases} \phi(x_j) = -\operatorname{dist}(\Gamma, \mathrm{x_j}) & \text{if } x_j \text{ is in } D, \\ \phi(x_j) = 0 & \text{if } x_j \text{ is at } \partial D, \\ \phi(x_j) = \operatorname{dist}(\Gamma, \mathrm{x_j}) & \text{if } x_j \text{ is outside } D. \end{cases}$$

Here, the functions g_α, k_α and ϕ are given in definitions (24), (25) and (26), respectively. This minimization problem is the topic of the next section.

3. The minimization problem

The purpose of this section is to bring forward a way to solve (27). Different techniques can be used to solve this minimization problem, and our approach is based on a gradient-type of method. Such a method requires all the partial derivatives of the involved cost-functional, i.e.

$$\frac{\partial J}{\partial p_1}, \frac{\partial J}{\partial p_2}, \ldots, \frac{\partial J}{\partial p_M}, \tag{31}$$

where J is defined in (27). Once the partial derivatives are found, the discrete level set function, $\phi(x) = \sum_{i=1}^{M} p_i N_i(x)$, is updated in the negative gradient direction. For all old parameter values, we will get new values by

$$\sum_{i=1}^{M} p_i^{\text{new}} N_i(x) = \sum_{i=1}^{M} p_i^{\text{old}} N_i(x) - \beta \sum_{i=1}^{M} \frac{\partial J}{\partial p_i}(p_1^{\text{old}}, p_2^{\text{old}}, \ldots, p_M^{\text{old}}) N_i(x), \tag{32}$$

using a fixed parameter β - see (26).

A critical task for all gradient-type of algorithms is the computation of the partial derivatives of the involved cost-functional. It is therefore in our interest to derive an effective method for computing the partial derivatives in (32). In fact, in the following we will show that all the partial derivatives of J can be computed by solving a single auxiliary problem. To do so, we study the weak form of the problem (28)-(29): Find v such that

$$\int_0^{t^*}\int_\Omega v_t \psi \, dx \, dt + \int_0^{t^*}\int_\Omega g_\alpha(\phi) I(v) \psi \, dx \, dt + \int_0^{t^*}\int_\Omega k_\alpha(\phi) \nabla v \cdot \nabla \psi \, dx \, dt = 0, \tag{33}$$

for all test functions $\psi \in V(\Omega)$, where $V(\Omega)$ denotes an appropriately defined space of functions[5].

3.1. Differentiation of the cost-functional. Recall the expression (26) for ϕ. Obviously, several different alternatives for discretizing such level set functions exist. Therefore, the task of determining the derivatives of J may, for the sake of convenience, be considered in a rather abstract setting. Such an approach was introduced by Tai and Chan in [5, 39] for various inverse problems. More precisely, they derived formulas for the Gateaux derivative of the involved cost-functionals with respect to level set functions. Furthermore, Tai and Chan pointed out that such abstract frameworks make it easy to reuse software and to differentiate the involved cost-functional with respect to a wide variety of parameters in the model. The approach proposed in [5, 39] is therefore well suited for various applications.

On the other hand, deriving a formula for the Gateaux derivative of J, as defined in (15), with respect to ϕ would certainly increase the technical level of the present text. Consequently, in the current more practical situation, we will focus

[5]More precisely, $V(\Omega) = L_2(0, t^*; H^1(\Omega))$, see [9] for further details.

on how to compute the derivatives of J with respect to the infarction parameters $p_1, p_2, \ldots, p_M$.

From (27) it follows that

$$\frac{\partial J}{\partial p_i} = -\int_0^{t^*}\int_{\partial\Omega} \big[d(x,t) - v(x,t;p_1,p_2,\ldots,p_M)\big] v_{p_i}(x,t;p_1,p_2,\ldots,p_M)\, dx\, dt. \tag{34}$$

Let $i \in \{1,2,\ldots,M\}$ be arbitrary and define $p = p_i$. We differentiate (33) with respect to p and find that

$$\begin{aligned}&\int_0^{t^*}\int_\Omega v_{pt}\psi\, dx\, dt + \int_0^{t^*}\int_\Omega g'_\alpha(\phi)\phi_p I(v)\psi\, dx\, dt + \int_0^{t^*}\int_\Omega g_\alpha(\phi) I'(v) v_p \psi\, dx\, dt \\ &\quad + \int_0^{t^*}\int_\Omega k'_\alpha(\phi)\phi_p \nabla v\cdot\nabla\psi\, dx\, dt + \int_0^{t^*}\int_\Omega k_\alpha(\phi)\nabla v_p\cdot\nabla\psi\, dx\, dt = 0,\end{aligned} \tag{35}$$

for all $\psi \in V(\Omega)$, and we use (24)-(25) to get

$$\begin{aligned}&\int_0^{t^*}\int_\Omega v_{pt}\psi\, dx\, dt + \int_0^{t^*}\int_\Omega g_\alpha(\phi) I'(v) v_p\psi\, dx\, dt + \int_0^{t^*}\int_\Omega k_\alpha(\phi)\nabla v_p\cdot\nabla\psi\, dx\, dt \\ &\quad = -\int_0^{t^*}\int_\Omega \delta_\alpha(\phi)\phi_p I(v)\psi\, dx\, dt - \int_0^{t^*}\int_\Omega (k_2-k_1)\delta_\alpha(\phi)\phi_p\nabla v\cdot\nabla\psi\, dx\, dt.\end{aligned} \tag{36}$$

Introducing the operator

$$a(\xi,\psi) = \int_0^{t^*}\int_\Omega \xi_t\psi\, dx\, dt + \int_0^{t^*}\int_\Omega g_\alpha(\phi) I'(v)\xi\psi\, dx\, dt + \int_0^{t^*}\int_\Omega k_\alpha(\phi)\nabla\xi\cdot\nabla\psi\, dx\, dt$$

for $\xi, \psi \in V(\Omega)$, equation (36) may be written on the form

$$a(v_p,\psi) = -\int_0^{t^*}\int_\Omega \Big(I(v)\psi + (k_2-k_1)\nabla v\cdot\nabla\psi\Big)\delta_\alpha(\phi)\phi_p\, dx\, dt, \quad \text{for all } \psi\in V(\Omega). \tag{37}$$

Next, let w denote the solution of the following auxiliary problem; find $w \in V(\Omega)$ such that

$$a(\psi,w) = -\int_0^{t^*}\int_{\partial\Omega} \big[d(x,t) - v(x,t;p_1,p_2,\ldots,p_M)\big]\psi(x,t)\, dx\, dt, \quad \text{for all } \psi\in V(\Omega). \tag{38}$$

By choosing $\psi = v_p$ in (38) we find from (34) that

$$\frac{\partial J}{\partial p} = a(v_p, w). \tag{39}$$

Further (37) and (39) imply that

$$\frac{\partial J}{\partial p} = -\int_0^{t^*}\int_\Omega \Big(I(v)w + (k_2-k_1)\nabla v\cdot\nabla w\Big)\delta_\alpha(\phi)\phi_p\, dx\, dt. \tag{40}$$

We thus conclude that the partial derivatives $\partial J/\partial p_1, \partial J/\partial p_2, \ldots, \partial J/\partial p_M$ of J can be computed by the following procedure;

a): Solve (33) for v
b): Solve (38) for w
c): For $i = 1,2,\ldots,M$, compute

$$\frac{\partial J}{\partial p_i} = -\int_0^{t^*}\int_\Omega \Big(I(v)w + (k_2-k_1)\nabla v\cdot\nabla w\Big)\delta_\alpha(\phi)\phi_{p_i}\, dx\, dt. \tag{41}$$

The complexity of this method is almost independent of the number M of infarction parameters. Only the number of integrals that must be computed in step **c**) increases as M grows. Hence, this is an efficient method for computing all the partial derivatives of J.

Note that the classical form of the adjoint problem (38) reads

$$-w_t + g_\alpha(\phi)I'(v)w = \nabla \cdot [k_\alpha \nabla w] \qquad \text{in } \Omega, \tag{42}$$

$$k_\alpha(\phi)\nabla w \cdot n = -(d - v) \qquad \text{along } \partial\Omega, \tag{43}$$

$$w(x, t^*) = 0 \qquad \text{in } \Omega. \tag{44}$$

3.2. An algorithm. Recall that the level set function ϕ, as well as the solutions v and w of (28)-(30) and (42)-(44), depend on the infarction parameters, i.e.

$$\begin{aligned}
\phi &= \phi(x; p_1, p_2, \ldots, p_M) = \phi(x; \mathbf{p}),\\
v &= v(x, t; p_1, p_2, \ldots, p_M) = v(x, t; \mathbf{p}),\\
w &= w(x, t; p_1, p_2, \ldots, p_M) = w(x, t; \mathbf{p}),
\end{aligned}$$

where $\mathbf{p} = (p_1, p_2, \ldots, p_M)^T$. Let $\mathbf{p}^n$, for $n = 0, 1, 2, \ldots$, denote approximations of the solution of the minimization problem (27). With this notation at hand, we propose the following algorithm for approximately solving (27);

Algorithm 1.

(1) *Choose an initial value v_0 for v to use in (30), as well as a suitable value for β in (32)*
(2) *Choose* $\mathbf{p}^0$
(3) *For $n = 0, 1, \ldots$ until convergence do*
   (a) *Solve (28)-(30) for $v^n = v(\mathbf{p}^n)$*
   (b) *Solve (42)-(44) for $w^n = w(\mathbf{p}^n)$*
   (c) *For $i = 1, 2, \ldots, M$ compute*

$$\frac{\partial J}{\partial p_i}(\mathbf{p}^n) = -\int_0^{t^*}\int_\Omega \Big(I(v^n))w^n + (k_2 - k_1)\nabla v^n \cdot \nabla w^n\Big)\delta_\alpha(\phi^n)\phi^n_{p_i}\, dx\, dt,$$

   where $\phi^n = \phi(\mathbf{p}^n)$, and $\phi^n_{p_i}$ denotes the partial derivative of ϕ^n with respect to p_i
   (d) *Update the infarction parameters by*

$$\mathbf{p}^{n+1} = \mathbf{p}^n - \beta\nabla J(\mathbf{p}^n),$$

   where $\nabla J(\mathbf{p}^n) = [\partial J/\partial p_1(\mathbf{p}^n), \partial J/\partial p_2(\mathbf{p}^n), \ldots, \partial J/\partial p_M(\mathbf{p}^n)]^T$

This algorithm is rather simple to implement, especially by utilizing the similarity between the discrete approximations of the forward and adjoint problems in steps 3 (a) and (b).

4. Regularization

Due to the ill-posed nature of the inverse problem (27), the process of identifying the size, shape and location of the infarction suffers from noise artifacts. Even worse, there may by several solutions that fit the same observation data. A general approach for addressing such kind of problems is to utilize a regularization term according to certain assumptions (typically derived from biological observations) for the region of interest. The results that deviate from these assumptions are penalized

by the regularization term, see [8]. For example, in [38] Chapter 7, they illustrate how noise artifacts could be reduced by the use of Tikhonov regularization for the involved minimization problems. However, for the level set framework introduced in sections 2.2-2.3, more common regularization approaches are to control the length of the interface ∂D between the healthy and ischemic regions, or to control the area inside (or outside) the interface [31, 3]:

$$|\partial D| = \int_\Omega |\nabla H_\alpha(\phi)|\, dx = \int_\Omega \delta_\alpha(\phi)|\nabla\phi|\, dx, \tag{45}$$

$$|D| = \int_\Omega (1 - H_\alpha(\phi))\, dx. \tag{46}$$

To determine a physically meaningful and stable solution, we approximately solve (27) by applying the following regularization; the area which is characterized as an infarcted region (where ϕ is negativ) should be minimized. With this approach we try to suppress all minor unconnected regions, that most likely are noise artifacts. Thus, we propose to minimize the following cost-functional

$$\begin{aligned} J\epsilon(p_1, p_2, \ldots, p_M) =& J(p_1, p_2, \ldots, p_M) + \epsilon \int_0^{t^*}\int_\Omega (1 - H_\alpha(\phi))\, dx\, dt \\ =& \frac{1}{2}\int_0^{t^*}\int_{\partial\Omega} \big[d(x,t) - v(x,t;p_1,p_2\ldots,p_M)\big]^2 dx\, dt \\ &+ \epsilon \int_0^{t^*}\int_\Omega (1 - H_\alpha(\phi))\, dx\, dt, \end{aligned} \tag{47}$$

where $\epsilon \geq 0$ is a parameter that controls the influence of the regularization term.

With this choice of regularization, we find that the partial derivatives of J_ϵ, for $i = 1, 2, \ldots, M$, to be given as

$$\begin{aligned} \frac{\partial J_\epsilon}{\partial p_i} =& \frac{\partial J}{\partial p_i} - \epsilon \int_0^{t^*}\int_\Omega \delta_\alpha(\phi)\phi_{p_i}\, dx\, dt \\ =& -\int_0^{t^*}\int_\Omega \Big(I(v)w + (k_2 - k_1)\nabla v\cdot\nabla w + \epsilon\Big)\delta_\alpha(\phi)\phi_{p_i}\, dx\, dt, \end{aligned} \tag{48}$$

where we have used (41). By comparing (41) with (48), it is easy to see how **Algorithm 1** can be modified in order to incorporate our choice of regularization, i.e. by involving ϵ in step 3 (c).

The performance of other choices of regularization methods should of course be evaluated as well. However, we regard the present work as a conceptual study of infarction modeling. The main focus of this paper is thus to introduce a suitable framework for infarction identification, and the key feature is to use the level set method to represent the interface between healthy and infarcted regions. To keep the discussion clean and simple, we have therefore investigated just a few, but essential, aspects of this ill-posed problem.

Clearly, different regularization and reinitialization methods, as well as techniques for approximating the Heaviside and Delta functions, etc., can have a major influence on the performance of numerical schemes. In fact, each of these factors induce several challenging problems, and it is consequently hard to illuminate all sides of these matters in the present text. The effect of using various regularization terms, is therefore not studied here, but we intend to give a thorough investigation of this issue in a follow-up paper.

5. Numerical examples

In this section we present some of the results obtained with the model described above. To evaluate the model with numerical examples, we first define a region D for (24)-(25), and let this region represent the infarcted area. The model (28)-(30) is thereafter used to generate ECG boundary measurements, denoted as observation data d. All knowledge of D is then put aside, and we try to recover the infarcted region by only using the observation data.

The principle behind our approach to determine D can be summarized as follows. We start by solving the forward problem (28)-(30) for an arbitrary chosen size, shape and location of an infarction, i.e. an arbitrary level set function ϕ. Thereafter, we solve the adjoint problem (42)-(44) using the same ϕ as in the forward problem. We then compute $\frac{\partial J_\epsilon}{\partial p_i}$, for $i = 1, 2, \ldots, M$, according to formula (48). In the end, all the infarction parameters are updated using a gradient-based approach to get new and more correct size, shape and location estimates for D. In the next iteration this new D (implicitly given by ϕ) is used as input when we solve the forward problem (28)-(30) again, and so on.

All the numerical experiments were carried out on an idealized heart geometry, i.e. on a square. A stimulus current, defining v_0 in the model (28)-(30), was applied inside the "heart" to activate the propagation of the electrical potential. The small bright region in the lower left corner of Figure 3(a) indicates the stimulus region.

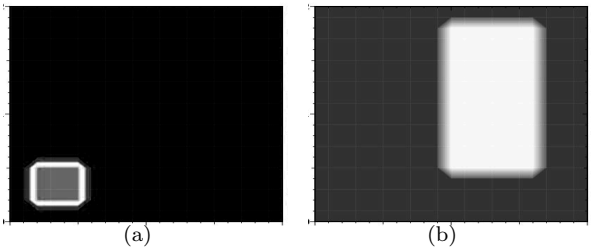

(a) (b)

FIGURE 3. An idealized heart geometry is represented by the dark square $\Omega = [0, 2] \times [0, 2]$. (a) The lower bright region represents the area in which stimulus current was applied. (b) The white rectangle indicates where we choose $\phi < 0$ initially, i.e. the initial guess for the infarcted area (the initial guess for the level set function ϕ). These two initial states were fixed throughout all the simulations presented in this paper.

In real life situations, the recorded membrane potential at the heart- or body surface will usually be corrupted by noise. To simulate this effect, we let $\tilde{d}(x_s, t_l) = d(x_s, t_l) + r(x_s, t_l)$ denote the corrupted measurements recorded at the boundary, in position x_s at time t_l. Here $r(x_s, t_l)$ is additive i.i.d[6]. zero-mean Gaussian noise that is uncorrelated in time. We let $s = 1, 2, \ldots, S$ and $l = 1, 2, \ldots, L$ be the discretization indices in space and time, respectively. For the numerical examples where we examine the effect of noisy observations, the following formula is used to indicate the relative error in the measurements

$$e = \frac{\sum_{s=1}^{S} \sum_{l=1}^{L} |r(x_s, t_l)|}{\sum_{s=1}^{S} \sum_{l=1}^{L} |d(x_s, t_l)|}. \tag{49}$$

[6]independent identically distributed

The parameter α in (23) controls the boarder-zone between healthy and infarcted tissues. For all the simulations, this parameter was fixed to one value; $\alpha = \frac{\Delta x}{2} = \frac{\Delta y}{2} = 0.2$. Concerning the constants in (25), we use the ratio $k_1 = \frac{k_2}{2}$ for the conductivity in damaged and healthy tissues, see [13, 36]. Finally, the parameter β in (32) is equal to 0.15 in all the computations presented below, cf. also steps 1 and 4(d) in **Algorithm 1**.

Example 1) We investigate the following trivial case: If no infarction is present, i.e. $D = \emptyset$, will the region covered by the initial guess shrink and finally disappear? This means that if observation data from a healthy heart is used, then no infarction should be found. Numerical tests where carried out both with and without noise present ($e = 0.1$, i.e. 10 % noise, and $e = 0.0$), and successful results were achieved for both cases in less than 10 iterations.

Example 2) We evaluate the ability to identify one infarction. The region covered by the infarction is given as the bright area in Figure 4(d). Our initial guess for this infarcted area is shown in Figure 3(b). A few results during the iteration process are given below in figures 4(a)-(c).

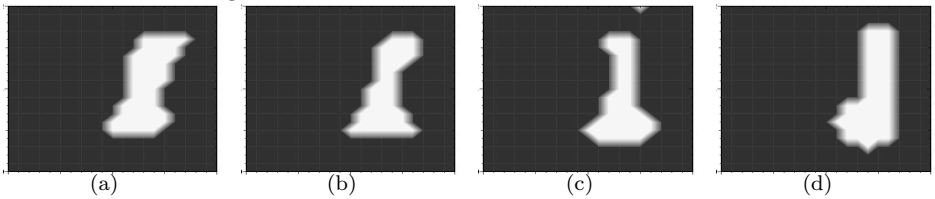

(a) (b) (c) (d)

FIGURE 4. Figures (a), (b) and (c) show estimates of the infarcted region after 4, 7, and 200 iterations, respectively. The unknown size, shape and location to detect is depicted in (d).

200 iterations were needed to get the algorithm to converge[7], and the estimate for D at convergence is shown in Figure 4(c). The size and location of D seem accurate, but details of the shape are missing. However, as mentioned in Section 4, several different solutions may fit the same observation data and therefore we can not expect to obtain a perfect match between the true D and the estimate for it.

Example 3) We repeat Example 2), but this time with noise corresponding to $e = 0.01$, $e = 0.05$ and $e = 0.10$ in the observation data, see (49). The final results obtained at convergence for this three different cases are depicted in figures 5(a)-(c).

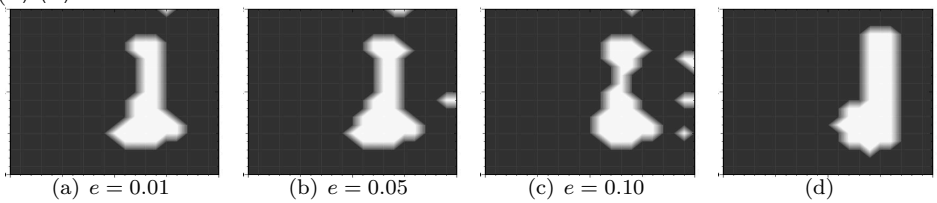

(a) $e = 0.01$ (b) $e = 0.05$ (c) $e = 0.10$ (d)

FIGURE 5. Figures (a), (b) and (c) contains approximations, computed from noisy observation data, of the "true" infarcted region shown in (d). Here, e represents the noise level defined in (49).

The regularization parameter ϵ in (48) was fixed to $\epsilon = 7$ for the three simulations in Example 3). The results above indicate that the proposed method is quite robust

[7]We terminated the iteration when $(\sum_{i=1}^{M} |\frac{\partial J_\epsilon}{\partial p_i}(\mathbf{p}^{n+1})|) \leq \frac{1}{50}(\sum_{i=1}^{M} |\frac{\partial J_\epsilon}{\partial p_i}(\mathbf{p}^{n})|)$.

with respect to noise. Even with a relative error as high as $e = 0.10$, i.e. 10 %, a fairly good estimate for D was obtained. By gradually increasing the noise level, the estimate for D gradually gets worse.

Example 4) We try to recover the two infarctions shown in Figure 6(d). This is a challenging task since our initial guess for D, depicted in Figure 3(b), now must split into two pieces, whereupon both pieces must be optimized with respect to size, shape and location. Fortunately, handling topological changes like splitting or merging of regions are trivial using the level set framework. A few results during the iteration process are given in figures 6(a)-(c). In this example, no noise were present in the observation data.

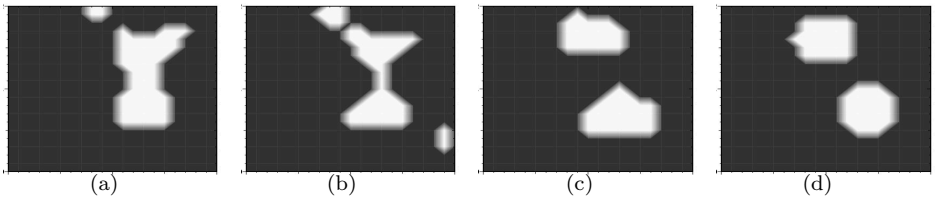

(a) (b) (c) (d)

FIGURE 6. (a)-(c) Estimates of the infarcted regions. More precisely, (a), (b) and (c) show the estimates after 10, 20 and 200 iterations, **Algorithm 1**, respectively. (d) The sizes, shapes and locations to detect in Example 4).

We want to emphasize that even if the level set framework is flexible, it cannot overcome the inherited ill-posedness of the problem (27). Therefore we cannot expect to obtain a perfect match between the unknown region D and the estimate for it in this example either. The sizes and locations of the two infarctions are found relatively accurate in Figure 6(c), but details concerning the shapes are missing.

Example 5) The same example as above, but now with relative errors $e = 0.01$, $e = 0.05$ and $e = 0.10$ in the observation data, see (49).

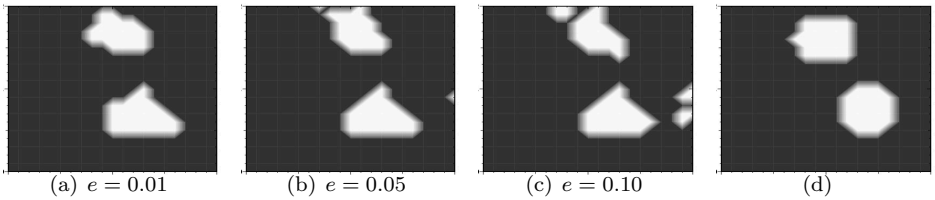

(a) $e = 0.01$ (b) $e = 0.05$ (c) $e = 0.10$ (d)

FIGURE 7. (a)-(c) Estimates of the infarcted region, using noisy observation data. (d) The unknown size, shape and location to detect in Example 5).

Only minor differences are visible when a relative observation error $e = 0.01$ is presented, compare Figure 6(c) and Figure 7(a). As in Example 3), we observe that the estimates of the infarcted regions get worse as the relative observation error increases. However, even with a noise level of $e = 0.1$, we manage to obtain some rough estimates of the infarcted areas.

Example 6) In the above examples only infarctions that cover relatively large regions of the "heart" were considered. The larger the infarctions are, the more impact they will have on the ECG recordings. Thus, large infarctions seem to be easier to detect than smaller ones. We therefore want to investigate if the proposed method is accurate enough to find an infarction that covers less than 1 percent of the heart.

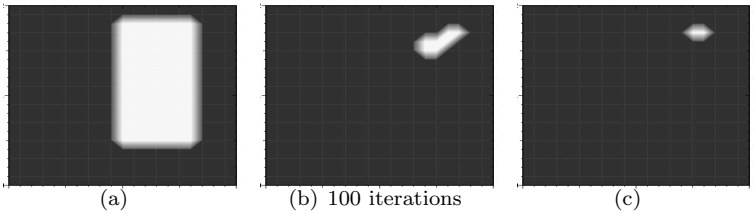

(a) (b) 100 iterations (c)

FIGURE 8. (a) Initial guess for the infarcted region. (b) Estimate for the infarcted region obtained by **Algorithm 1**. (c) The unknown size, shape and location to recover.

Starting from an initial guess, as shown in Figure 8(a), successive adjustments to the infarcted region produce an estimate as depicted in Figure 8(b). The "true" physical characteristics of the ischemic area considered in this case is shown in Figure 8(c). As expected, it was hard to get a proper estimate for this small infarction. Comparing Figures 8(b) and (c), we see that the size of the approximated infarction, produced by **Algorithm 1**, was over-estimated in this challenging test.

6. Conclusions

The purpose of this paper has been to investigate the possibilities for identifying heart infarctions by utilizing a level set framework. A modified Monodomain model along with an output least squares formulation, that compares simulation results with observation data, were used. A very simplified heart geometry was considered, and only 2D experiments were carried out.

The numerical experiments substantiate that, for our rather simple cases, the proposed method manage to solve this complicated inverse problem. Moreover, the level set framework possess the flexibility to recover the characteristics of infarctions, even for regions with rather irregular geometries.

In our future work we intend to test our scheme on realistic heart geometries, as well as on more accurate mathematical models. That is, on models involving both the Bidomain equations and complex models for the cell dynamics. An important part of this work will be to improve the efficiency of **Algorithm 1**.

References

[1] H. T. Banks and K. Kunisch, *Estimation Techniques for Distributed Parameter Systems*, Birkhäuser, 1989.

[2] Y. Birnbaum and B. J. Drew, *The electrocardiogram in st elevation acute myocardial infarction: correlation with coronary anatomy and prognosis*, Postgrad. Med. J., 79 (2003).

[3] M. Burger and S. Osher, *A survey on level set methods for inverse problems and optimal design*, CAM-Report 04-02, (2004).

[4] T. Chan and L. Vese, *Active contours without edges*, IEEE Trans. Image Processing, 10 (2001), pp. 266–277.

[5] T. F. Chan and X.-C. Tai, *Level set and total variation regularization for elliptic inverse problems with discontinuous coefficients*, Journal of Computational Physics, 193 (2003), pp. 40–66.

[6] E. T. Chung, T. F. Chan, and X.-C. Tai, *Electrical impedance tomography using level set representation and total variational regularization*, J. Comput. Phys, (2004). online.

[7] O. Dössel, *Inverse problem of electro- and magnetocardiography: Review and recent progress*, International Journal of Bioelectromagnetism, 2 (2000).

[8] H. W. Engl, M. Hanke, and A. Neubauer, *Regularization of Inverse Problems*, Kluwer Academic Publishers, 1996.

[9] L. C. Evans, *Partial Differential Equations*, American Mathematical Society, 1998.

[10] P. C. Franzone, B. Taccardi, and C. Viganotti, *An approach to inverse calculation of epicardial potentials from body surface maps*, Adv.Cardiol, 21 (1978), pp. 50–54.
[11] F. Greensite and G. Huiskamp, *An improved method for estimating epicardial potentials from the body surface*, IEEE Transactions on Biomedical Engineering, 45 (1998), pp. 98–104.
[12] C. W. Groetsch, *Inverse Problems in the Mathematical Sciences*, Vieweg, 1993.
[13] F. Hanser, M. Seger, B. Tilg, R. Modre, G. Fisher, B. Messnarz, F. Hintringer, T. Berger, and F. X. Roithinger, *Influence of ischemic and infarcted tissue on the surface potential*, Computers in Cardiology, 30 (2003), pp. 789–792.
[14] C. S. Henriquez, *Simulating the electrical behaviour of cardiac tissue using the bidomain model*, Crit. Rev. Biomed. Eng., 21 (1993), pp. 1–77.
[15] R. P. Holland and H. Brooks, *Precordial and epicardial surface potentials during myocardial ischemia in the pig*, Circ. Res., 37 (1975), pp. 471–480.
[16] B. Hopenfeld, J. Stinstra, and R. Macleod, *A mechanism for st depression associated with contiguous subendocardial ischemia*, Journal of Cardiovascular Electrophysiology, 15 (2004).
[17] P. Hunter, P. McNaughton, and D. Noble, *Analytical models of propagation in the excitable cells*, Prog Biophys Mol Biol, 30 (1975), pp. 99–144.
[18] P. R. Johnston, *A cylindrical model for studying subendocardial ischemia in the left ventricle*, Math. Biosci., 186 (2003), pp. 43–61.
[19] P. R. Johnston, D. Kilpatrick, and C. Y. Li, *The importance of anisotropy in modeling st segment shift in subendocardial ischaemia*, IEEE Trans. Biomed. Eng., 48 (2001), pp. 1366–1376.
[20] J. Keener and J. Sneyd, *Mathematical Physiology*, Springer-Verlag, 1998.
[21] D. Kilpatrick, P. R. Johnston, and D. S. Li, *Mechanisms of st change in partial thickness ischemia*, J. Electrocardiol., 36 (2003), pp. 7–12.
[22] J. Lau, J. P. Ioannidis, E. M. Balk, C. Milch, N. Terrin, P. W. Chew, and D. Salem, *Diagnosing acute cardiac ischemia in the emergency department: a systematic review of the accuracy and clinical effect of current technologies*, Ann. Emerg. Med., 37 (2001), pp. 453–460.
[23] D. Li, C. Y. Li, A. C. Yong, and D. Kilpatrick, *Source of electrocardiographic st changes in subendocardial ischemia*, Circ. Res., 82 (1998), pp. 957–970.
[24] G. T. Lines, M. L. Buist, P. Grøttum, A. J. Pullan, J. Sundnes, and A. Tveito, *Mathematical models and numerical methods for the forward problem in cardiac electrophysiology*, Computations and Visualization in Science, 5 (2003), pp. 215–239.
[25] G. T. Lines, P. Grøttum, and A.Tveito, *Modeling the electrical activity of the heart: a bidomain model of the ventricles embedded in a torso*, Comput. Vis. Sci., 5 (2003), pp. 195–213.
[26] M. MacLachlan, J. Sundnes, and G. Lines, *Simulation of st segment changes during subendocardial ischemia using a realistic 3d cardiac geometry*, submitted, (2004).
[27] R. S. MacLeod and D. H. Brooks, *Recent progress in inverse problems in electrocardiology*, IEEE Engineering in Medicine and Biology, 17 (1998), pp. 73–83.
[28] W. T. Miller and D. B. Geselowitz, *Simulation studies of the electrocardiogram I. the normal heart*, Circ. Res, 43 (1978), pp. 301–315.
[29] ———, *Simulation studies of the electrocardiogram: II. ischemia and infarction*, Circ. Res., 43 (1978), pp. 315–323.
[30] S. Osher and R. Fedkiw, *Level set methods: An overview and some recent results*, J: Comput. Phys., 169 (2001), pp. 463–502.
[31] S. Osher and R. Fedkiw, *Level Set Methods and Dynamic Implicit Surfaces*, Springer-Verlag, 2002.
[32] S. Osher and F. Santosa, *Level set methods for optimization problems involving geometry and constraints. I. frequencies of a two-density inhomogeneous drum.*, J. Comput. Phys, 171(1) (2001), pp. 272–288.
[33] S. Osher and J. Sethian, *Fronts propagating with curvature-dependent speed: Algorithms based on Hamilton-Jacobi formulations*, Journal of Computational Physics, 79 (1988), pp. 12–49.

[34] D. Schwartzman, I. Chang, J. Michele, M. Mirotznik, and K. Foster, *Electrical impedance properties of normal and chronically infarcted left ventricular myocardium*, Journal of Interventional Cardiac Electrophysiology, 3 (1999), pp. 213–224.

[35] J. A. Sethian, *Level set methods and fast marching methods*, vol. 3 of Cambridge Monographs on Applied and Computational Mathematics, Cambridge University Press, Cambridge, second ed., 1999. Evolving interfaces in computational geometry, fluid mechanics, computer vision, and materials science.

[36] J. Stinstra, B. Hopenfeld, and R. Macleod, *A model of the passive cardiac conductivity*, International Journal of Bioelectromagnetism, 5 (2003), pp. 185–186.

[37] J. Sundnes, G. Lines, K.-A. Mardal, and A. Tveito, *Multigrid block preconditioning for a coupled system of partial differential equations modeling the electrical activity in the heart*, Computer Methods in Biomechanics and Biomedical Engineering, 5 (2002), pp. 397–409.

[38] J. Sundnes, G. L. Lines, X. Cai, B. F. Nielsen, K. A. Mardal, and A. Tveito, *Computing the Electrical Activity in the Human Heart*, Accepted for publication, 278 pages, Springer-Verlag, 2004.

[39] X.-C. Tai and T. Chan, *A survey on multiple level set methods with applications for identifying piecewise constant functions*, International J. Numer. Anal. Modeling, 1 (2004), pp. 25–48.

[40] L. Tung, *A Bi-domain model for describing ischemic myocardial D-C potentials*, PhD thesis, MIT, Cambridge, 1978.

Department of Scientific Computing, Simula Research Laboratory, Martin Linges vei 17, Fornebu, P.O. Box 134 NO-1325 Lysaker, Norway.

E-mail: mariul@simula.no and bjornn@simula.no

URL: http://www.simula.no/people